Targeting EWSR1-FLI1 oncogene induced protein kinase C beta abolishes Ewing sarcoma growth in vivo

Didier Surdez[1,2], Magdalena Benetkiewicz[1,2], Virginie Perrin[1,2], Zhi-Yan Han[1,2], Gaëlle Pierron[1,3], Stelly Ballet[1,3], François Lamoureux[4,5], Françoise Rédini[4,5], Estelle Daudigeos-Dubus[6,7], Birgit Geoerger[6,7], Olivier Delattre[1,2,3] and Franck Tirode[1,2,*]

[1] Institut Curie, 26 rue d'Ulm, 75248 Paris cedex 05, France

[2] INSERM U830, Unité de Génétique et Biologie des Cancers, Paris, France

[3] Institut Curie, Unité de génétique somatique, Paris, France

[4] LUNAM Universités, Université de Nantes, EA3822 : Laboratoire de Physiopathologie de la Résorption Osseuse et Thérapie des Tumeurs Osseuses Primitives, Nantes, France

[5] INSERM, UMR 957, Nantes, France

[6] Institut Gustave Roussy, Université Paris-Sud XI, 114 rue Edouard Vaillant, 94805 Villejuif, France

[7] Centre National de Recherche Scientifique (CNRS), Laboratoire de Vectorologie et Thérapeutiques Anticancéreuses, UMR 8203, 91405 Orsay, France

Running title: Roles of PRKC in Ewing sarcoma's biology

Keywords: Ewing sarcoma / EWSR1-FLI1 / Protein Kinase B / apoptosis / xenograft

* Corresponding author :
Franck Tirode
Unité de Génétique et Biologie des Cancers, INSERM U830, Section de Recherche, Institut Curie, 26 rue d'Ulm, 75248 Paris Cedex 05
Tel: 33 1 56 24 66 83
Fax: 33 1 56 24 66 30
Email : franck.tirode@curie.fr

Grant Support
This work was supported by grants from the Institut National de la Santé et de la Recherche Médicale (FL,FR,OD,FT), the Centre National de la Recherche Scientifique (EDD,BG), the Institut Curie (DS,MB,VP,ZHY,GP,SB), the Institut National du Cancer (DS :SYBEwing project: 2009-1-PLBIO-04 and FT,VP :BORTES project : 2008-PLBIO-06), the Ligue Nationale contre le Cancer (Equipe labellisée and CIT program), the Réseau National des Génopoles, Agence National de la Recherche, the European Union (MB : KCK and EET pipeline programs), the société Française des Cancers de l'Enfant, and the following associations: Courir pour Mathieu, Dans les pas du Géant, Olivier Chape, Les Bagouzamanon and les Amis de Claire.

Authors declare no conflict of interest

Word count: 4628. 6 main figures, 3 supplemental figures and 2 supplemental materials are included

Abstract

Identification of druggable targets is a prerequisite for developing targeted therapies against Ewing sarcoma. We report the identification of Protein Kinase C Beta (PRKCB) as a protein specifically and highly expressed in Ewing sarcoma as compared to other pediatric cancers. Its transcriptional activation is directly regulated by the EWSR1-FLI1 oncogene. Getting insights in PRKCB activity we show that, together with PRKCA, it is responsible for the phosphorylation of histone H3T6, allowing global maintenance of H3K4 trimethylation on a variety of gene promoters. In the long term, *PRKCB* RNA interference induces apoptosis *in vitro*. More importantly, in xenograft mice models, complete impairment of tumor engraftment and even tumor regression were observed upon PRKCB inhibition, highlighting PRKCB as a most valuable therapeutic target. Deciphering PRKCB roles in Ewing sarcoma using expression profiling, we found a strong overlap with genes modulated by EWSR1-FLI1 and an involvement of RPKCB in regulating crucial signaling pathways. Altogether, we show that PRKCB may have two important independent functions and should be considered as highly valuable for understanding Ewing sarcoma biology and as a promising target for new therapeutic approaches in Ewing sarcoma.

Introduction

Ewing sarcoma (ES) is the second most frequent childhood bone tumor. Clinically, ES is a highly metastatic tumor with around 25% of patients presenting metastasis at the time of diagnosis. Although great advances have been made in the treatment of local disease, therapies used for advanced stages of the disease are still disappointing, the five year overall survival still being critically low. Thus the discovery of novel druggable targets allowing targeted therapies is mandatory.

Since the discovery and characterization of the causal translocation event (1; 2), researches were driven by the quest for targets of the chimeric EWSR1-FLI1 transcription factor, the main oncogenic event in more than 85% of ES. Most of the studies aiming at identifying important molecules involved in ES oncogenesis were based either on EWSR1-FLI1 inhibition in Ewing sarcoma cells or EWSR1-FLI1 expression in non-Ewing cell lines. Thus, many different studies, including ours, identified genes involved in EWSR1-FLI1-dependent cell survival, such as IGF-1R (3) and IGFBP (4; 5), PPP1R1A (6), MK-STYX/STYXL1 (7), NR0B1 (8; 9), NKX2-2 (10), GSTM4 (11) and SOX2 molecules (12). Proposed as a promising targeted therapy, IGF signaling inhibition has been extensively investigated in the context of Ewing sarcoma and several clinical trials have been conducted. Although well tolerated, several reports of phase II studies suggested that only about one patient out of four would benefit from IGF-1R monoclonal antibodies as single therapy (13). On the other hand, some studies analyzed primary tumors to find specific gene signature of Ewing sarcoma (6; 14–16).

Aiming at finding genes that are specifically found in primary Ewing tumors compared to other tumors types and modulated by EWSR1-FLI1, we identified the protein kinase C beta (PRKCB). In the context of ES, we demonstrate here that PRKCB is crucial for cell survival *in vitro* and tumor development *in vivo*. We demonstrate that inhibition of PRKCB induces apoptosis and stimulates TNF and NF-kB signaling and that concomitant inhibition of both

PRKCA and PRKCB, by pharmacological inhibition or RNA silencing is required to decrease histone H3 lysine 4 methylation levels.

Materials and Methods

Microarrays and statistical analysis. Ewing tumors samples (GSE34620) together with samples of other pediatric or bone tumors including 32 small round cell desmoplastic tumors, 52 medulloblastomas (GSE12992), 64 neuroblastomas (GSE12460), 122 rhabdomyosarcoma (20), 27 osteosarcomas (GSE14827) and 34 synovial sarcomas (GSE20196) were used for this analysis. All microarray data were simultaneously normalized using the gcrma package version 2.18.1 in R 2.10.1 environment (34). BGA analyses were completed using made4 R package (35). For siRNA inhibition microarrays, A673 cells were transfected by the indicated siRNA and harvested 72hours post transfection. Total RNAs were extracted using Trizol Reagent and processed on Affymetrix HuGene1.1STv1 GeneChip microarrays. RMA normalization was performed using Brainarray Entrez gene CDF v14.1 (36) in R environment. Group comparisons were done using Welch Two Sample t-test statistic and DAVID gene ontology analyses (37) were performed online (http://david.abcc.ncifcrf.gov/home.jsp). Gene set enrichment analysis (38) was done by comparing siPRKCB and siControl samples using a log ratio of classes metric.

***In vivo* mice experiments**. For A673-shPRKCB463_B5M3 xenograft tumors in SCID mice**,** twenty millions cells resuspended in 200 µl of PBS were injected subcutaneously in the flank of five-weeks-old severe combined immunodeficient (SCID) female mice (Charles River laboratories, Les Arbresles, France). Doxycycline was added to the drinking water at 2 mg/mL together with 5% sucrose. Tumor volume was determined by caliper measurements every 2-3 days until volume reached 1500mm^3. For the A673 xenograft Ewing sarcoma model in nude mice, twenty millions cells were injected next to the tibia of four-week-old male athymic mice (Janvier, L'Arbresles, France) under anesthesia [inhalation of a combination of isoflurane/ air (1.5%, 1 L/min) and buprenorphine (0.05 mg/kg; Temgésic, Schering-Plough)]. Once tumors were measurable, mice were randomly assigned into treatment groups receiving either oral gavage with enzastaurin suspended in olive oil (100mg/kg, twice daily; n

= 6) or oral vehicle alone (n = 7). Tumor volume was measured three times a week (length × width × depth × 0.5432). The mice were sacrificed by CO2 inhalation when the tumor volume exceeded 3,000 mm^3. Experiments were performed in accordance with recommendations of the European Community (86/609/EEC), the French Competent Authority and with the institutional guidelines of the French Ethical Committee (CEEA.PdL.06).

Chromatin immunoprecipitation. For *PRKCB* promoter CHIP, experiments were carried out as previously described (39) using either C19 or 7.3 FLI1 antibodies except that one microliter of CHIP DNA was amplified for 30 cycles by PCR amplification (Applied Biosystems) using *PRKCB* promoter-specific primers (-428/-270 region before TSS). For Histone ChIP, experiments were conducted using the MAGnify Chromatin Immunoprecipitation system (Invitrogen) using 3 µg of DNA and 2 µg of antibody per ChIP, and following manufacturer's recommandations. CHIP DNA was amplified using quantitative PCR (Applied Biosystems) using primers specific for H3K4 trimethylated regions around 19 gene's TSS. H3K4 trimethylated regions were selected according to their profile in the ENCODE Promoter-Associated Histone Mark (H3K4Me3) on 9 Cell Lines dataset (26).

Additional experimental details are available in the SOM .

Results

PRKCB is strongly over-expressed in Ewing tumors

To find specific genes expressed in Ewing sarcoma, a supervised Between Group Analysis (17) was performed comparing expression profiles of 39 Ewing tumors samples with those of other pediatric tumors including 32 small round cell desmoplastic tumours, 52 medulloblastomas (18), 64 neuroblastomas (19) and 122 rhabdomyosarcoma (20) (Figure 1A). Among the top 100 probesets found to be specific for ES (see supplemental table S1) several represented genes that were previously identified as important for Ewing tumors like NKX2-2 (10), NR0B1 (8; 9), LIPI (21), DKK2 (22) or XG (23) and most of them were previously identified as EWSR1-FLI1-dependent genes (4; 15; 24). Among these genes we focused our attention on the protein kinase C beta (*PRKCB*) for which five probesets (Figure 1A) were significantly overexpressed in Ewing tumors as compared to other pediatric or bone tumors (Figure 1B). Indeed, mean value of *PRKCB* expression in Ewing tumors is 13 fold superior to mean value of the closest group (neuroblastomas). Although two isoforms of *PRKCB* (*PRKCB1* and *PRKCB2*) distinguished by their differentially spliced last exon have been described (hereafter we will indicate *PRKCB* when referring to both isoforms), *PRKCB2* is the predominant isoform in ES as compared to other non-Ewing cancer cell lines (Figure 1C). Strong *PRKCB* overexpression thus appears to be highly specific of Ewing tumors.

PRKCB expression is directly dependent on EWSR1-FLI1

Inhibition of EWSR1-FLI1 using siRNA in A673, EW24 and SK-N-MC Ewing cell lines dramatically reduced PRKCB expression levels at both RNA and protein levels (Figure 2A and 2B), indicating that PRKCB expression in ES cells is EWSR1-FLI1 dependent. To assess the direct role of EWSR1-FLI1 in PRKCB expression, luciferase reporter experiments with *PRKCB* promoter (from -1147 to +22 according to transcription start site) were conducted. As shown on figure 2C, ectopic expression of EWSR1-FLI1 in HeLa cell line

strongly increased luciferase activity. In addition, in shA673-1C cell line, which allows a doxycycline-mediated inhibition of EWSR1-FLI1 (24), *PRKCB* promoter activity was significantly decreased upon EWSR1-FLI1 inhibition (Figure 2D). Finally, chromatin immunoprecipitation by two different EWSR1-FLI1 antibodies conducted in A673 cells indicated the presence of EWSR1-FLI1 within the *PRKCB* promoter *in vivo* (Figure 2E). These different results clearly indicate that EWSR1-FLI1 is directly responsible for the high expression of PRKCB in Ewing cell lines.

PRKCB is an active kinase in ES and is responsible for histone H3T6 phosphorylation

In a recent publication on prostate cancer cells (25), PRKCB was shown to phosphorylate histone H3 on its threonine 6 (H3T6ph) leading to a decreased ability for the cell to remove di/tri-methyl tags on lysine 4 of H3 (H3K4me2/me3). We therefore investigated in Ewing sarcoma if PRKCB overexpression correlated with high H3T6 phosphorylation –and consequently H3K4 methylation– levels and if his effect was related to EWSR1-FLI1 direct DNA binding. Promoter regions of thirteen known EWSR1-FLI1 modulated genes (7 induced: *AURKB, CAV1, CCND1, EZH2, NKX2.2, NR0B1, TERT* and 6 repressed: *DKK1, IGFBP3, IGFBP5, RUNX2, TGFBI, TGFBR2*) and 6 unmodulated genes (*CREBBP, ENSA, MAST2, PDPK1, ROCK1, SNF8*) were selected according to their profile in the ENCODE Promoter-Associated Histone Mark (H3K4Me3) on a 9 cell lines dataset (26). In order to study the effect of PRKCB inhibition on H3T6 phosphorylation, we treated A673 cells for 72 hours with Enzastaurin (an inhibitor of PRKCB, Graff et al., 2005) or with equivalent amount of DMSO as a control condition. Chromatin immunoprecipitation (ChIP) were then performed using antibody against H3T6ph, H3K4me3 or control IgGs. An almost global decrease of H3T6ph level and a massive reduction of H3K4me3 level on both EWSR1-FLI1 modulated and unmodulated genes were observed upon Enzastaurin treatment (Figure 3A-B). To confirm this inhibition effect, we silenced *PRKCB* by siRNA in A673 for 72h and compared it to control siRNA conditions. To our surprise, inhibition of *PRKCB* did not significantly affect

H3T6ph or H3K4me3 levels (Figure 3C-D). To account for this result, we hypothesized that other members of classical PKCs subfamily may complement PRKCB deficiency. PRKCA is of particular interest as it shares high structural and functional homology with PRKCB. For instance both PRKCB and PRKCA can phosphorylate H3T6 *in vitro* (25). Additionally, although Enzastaurin is a specific PRKCB inhibitor (IC50: 6nM) it also clearly displays inhibitory effect against PRKCA (IC50: 39nM) (27). Consequently, since PRKCA is also expressed in Ewing cell lines (28) and personal observation), we hypothesized that either PRKCA or PRKCB could be sufficient to maintain H3T6ph and H3K4me3 levels. ChIP experiments were then performed in A673 cells transfected either with siPRKCB or siPRKCA alone or with both siRNAs. As postulated, only the combinatorial inhibition of *PRKCA* and *PRKCB* led to a drastic reduction of H3T6 phosphorylation and H3K4 trimethylation levels (Figure 3E-F) whereas inhibition of *PRKCA* alone did not decrease H3K4me3 (supplemental Figure S1). Altogether we demonstrate here that PRKCB is responsible, together with PRKCA, for maintaining steady state H3T6ph and H3K4me3 levels, at least on most of tested promoters.

PRKCB is crucial for Ewing cell survival *in vitro*

Knowing that PRKCB was active in ES cells, we next investigated whether PRKCB expression was necessary for cell survival. For this purpose A673, SK-N-MC and TC71 cell lines were infected with lentiviral particles containing shRNAs against *PRKCB* (sh463 and sh847 are located 463nt and 847nt downstream of transcription start site according to NM_002738.3, respectively) that elicited strong *PRKCB* inhibition (supplemental Figure S2A). Five days after infection, inhibition of *PRKCB* induced a dramatic decrease in proliferation rate in all three Ewing cell lines (Figure 4A). To exclude shRNA off-target effect hypothesis, phenotypical rescue experiments were conducted by re-expressing *PRKCB1* or *PRKCB2* carrying synonymous mutations within their shRNA-targeted sequence ($PRKCB^{463m}$ and $PRKCB^{847m}$, supplemental Figure S2B-C). In *PRKCB*-silenced cells, restoration of

PRKCB expression completely rescued their growth capacities (Figure 4B), thus excluding off-target effects and confirming the specificity of the shRNA-induced phenotypes. To unravel mechanisms of growth inhibition observed upon *PRKCB* inhibition, we investigated cell cycle phases and apoptosis pathways. Cell cycle analysis using BrdU incorporation did not show any significant differences in G1, S or G2/M phases between control and *PRKCB* knock-down condition. In contrast, a strong increase of the subG1 fraction was observed (Figure 4C). Investigation of caspase 3 cleavage and annexin V presentation confirmed that *PRKCB* inhibition in three different cell lines significantly increased apoptosis (Figure 4C). As several compounds have been previously reported to specifically inhibit protein kinase C beta activity, we investigated whether pharmacological PRKCB inhibition was also effective in ES. We choose to investigate Enzastaurin (27) as this molecule has been fostered to phase II/III clinical trials for several diseases. Growing Ewing sarcoma A673, SK-N-MC and TC71 cell lines with increasing amount of Enzastaurin led to a dramatic reduction of cell viability with an IC50 around 5 µM. (Figure 4D). Altogether, these results indicate that *in vitro* inhibition of PRKCB strongly induces cell death via apoptotic pathways.

PRKCB inhibition induces tumor regression *in vivo*

We next wondered whether we could recapitulate *in vivo* the tremendous apoptotic effect of *PRKCB* inhibition observed *in vitro*. For this purpose, we generated the shA673-B5M3 Ewing cell line that expresses the shRNA463 directed against *PRKCB* under the control of a doxycycline inducible promoter (supplemental Figure S3). Xenograft tumors were then raised into SCID mice by subcutaneously implanting shA673-B5M3 cells or control cells (shA673-pTER). Remarkably, shA673-B5M3 xenograft tumor growth was completely abolished when mice were treated with doxycycline as soon as four days after cells inoculation (Figure 5A). Moreover, shRNA-mediated *PRKCB* inhibition reduced tumor size very significantly when mice were doxycycline-treated once tumors were detectable (Figure 5B). Finally, A673 cells were injected at the bone periphery, into mouse tibial muscle, to mimic the human disease.

In these mice, treatment with Enzastaurin led to a significant reduction of tumor growth (Figure 5C). Overall, these three *in vivo* experiments clearly demonstrated that blocking PRKCB prevents Ewing sarcoma tumor engraftment, reduces tumor growth and promotes tumor reduction.

Roles of PRKC in Ewing sarcoma

We showed that pharmacological inhibition of PRKC led to a decreased histone phosphorylation and that PRKB inhibition led to apoptosis but it is unlikely that these two mechanisms are related since PRKCB inhibition had no effect on histone modification. Thus, to trying to decipher the molecular roles of PRKCB in Ewing sarcoma we performed expression profiling on A673 Ewing cell lines treated by specific siRNA against either PRKCB or EWSR1-FLI1 and with a non-targeting siRNA as control. Supervised differential analyses between samples treated by either specific siRNAs and samples treated with the control siRNA were performed and the lists of genes modulated in the different conditions were compared to each other (Figure 6A and supplemental table S2). As expected, we found down-regulation of many histones/chromatin/chromosome organization gene categories reinforcing the possible link between EWSR1-FLI1 and chromatin remodeling through PRKCB (supplemental table S3). More striking, we observed an extremely significant overlap while comparing EWSR1-FLI1 and PRKCB modulated genes. Indeed, more than half of the genes modulated upon PRKCB inhibition were also modulated during EWSR1-FLI1 inhibition (Figure 6A). Looking at the gene ontology or pathways modulated by either siRNA inhibition (see supplemental table S3), cell death was significantly up-regulated, which was consistent with the observed phenotype. Indeed, during PRKCB inhibition, caspase 3, caspase 8 and TNFRSF12A (Tweak-receptor) were strongly up regulated and are known to induce apoptosis in some tumors (29). Furthermore, gene set enrichment analyses demonstrated that PRKCB inhibition led to a significant increase of TNF and NF-kB pathways, also possibly leading to apoptosis (Figure 6B). Altogether, our results demonstrate that PRKCB possesses

at least two different functions in Ewing sarcoma, the first being its involvement in crucial signaling pathways leading to rapid cell death when impaired, the second being its responsibility for histone H3T6 phosphorylation, leading to long term impact on transcriptional activity.

Discussion

We identified PRKCB as a major Ewing specific protein, which overexpression is directly linked to EWSR1-FLI1. Indeed, bioinformatics approaches led to the identification of *PRKCB* among the most overexpressed gene in Ewing sarcomas, which could be confirmed using quantitative RT-PCR. Moreover, using siRNA inhibition experiments we show here a direct regulation of *PRKCB* expression by EWSR1-FLI1 that is validated by ChIP and luciferase reporter promoter experiments. Noticeably, vascular endothelial growth factor (VEGF) was recently shown to stimulate *PRKCB* expression in chronic lymphocytic leukemia cells (30). It is notable that ES patients display increased serum VEGF levels as compared with healthy controls (31). Thus, direct and indirect activation of *PRKCB* through respectively EWSR1-FLI1 and VEGF signaling may converge to increase expression level of PRKCB in ES.

As overexpression is not necessarily correlated with increased activity, we investigated whether PRKCB was active. Numerous potential PRKCB substrates have been described in the literature such as AKT (Graff et al., 2005) and Bcl2 or BimEL (zum Buschenfelde et al., 2010), but we focused our attention on histone H3T6 phosphorylation. Interestingly enough, we show that inhibition of *PRKCB* is not sufficient to modify H3T6 phosphorylation pattern on a selected set of genes. Eventually, we demonstrate here that either PRKCB or PRKCA expression is sufficient to prevent histone H3K4 demethylation in ES since *PRKCB* and *PRKCA* should be inhibited together to see an effect on histone H3T6 phosphorylation, therefore indicating a redundant function. Nevertheless we cannot rule out a peculiar effect of PRKCB on specific promoters that were not tested here. In prostate cancer cells, upon treatment with R1881 -a synthetic agonist of the androgen receptor-, Metzger et al. have shown that PRKCB was able to phosphorylate H3T6 only in the promoter region of androgen responsive genes. A similar mechanism could be involved in ES. Despite the lack of a direct interaction observation, we could hypothesize a process in which PRKCB interacts, directly

or not, with EWS-FLI1 on a restricted set of promoter, leading to either transcriptional activation or repression of the corresponding genes.

Expression profiling experiments showed a strong overlap between genes modulated upon EWSR1-FLI1 knock-down and those modulated by PRKCB inhibition. To account for this result, two hypotheses could be made: i) PRKCB may directly phosphorylate EWSR1-FLI1 therefore affecting its activity or stability. However, preliminary experiments did not allow us to detect PRKCB driven EWSR1-FLI1 phosphorylation but more sophisticated experiments are required. ii) PRKCB may induce chromatin modification of many EWS-FLI1 target genes. However, we show that both PRKCA and PRKCB are expressed in ES and that they share redundant functions on H3T6 phosphorylation, leading to a more complex regulation of chromatin status as originally thought.

We also demonstrate here that *PRKCB* is a major therapeutic target in Ewing sarcoma. Indeed, inhibition of PRKCB either by small molecules inhibitors or by siRNA induces apoptosis. Therefore, PRKCB inhibition in Ewing cell lines has rather a cytotoxic than a cytostatic effect that is of strong interest for therapeutic use. Furthermore, specific shRNA inhibition of *PRKCB* is sufficient to impair tumorigenesis of Ewing cells *in vivo*. To our knowledge and apart from *EWSR1-FLI1* inhibition (32), this is the first demonstration of a single gene knockdown leading tumor shrinkage in Ewing xenograft models, opening interesting therapeutic opportunities based on PRKCB extinction. Usage of specific drugs such as Enzastaurin also proved its efficacy for inhibiting tumor growth *in vivo* but to a lesser extent than with RNA inhibition. Accounting for this result, Enzastaurin accumulation in mice adipose tissue was observed in these experiments (data not shown) leading to its reduced bioavailability at tumor sites.

In this study, we clearly demonstrated the anti-apoptotic properties of PRKCB in the context of ES, as its inhibition is sufficient to robustly trigger apoptosis. To account for this effect, microarray data indicate a significant increase of TNF superfamily death receptor upon

PRKCB silencing. Indeed, TNFRSF12A (TWEAK receptor), TNFRSF10A and TNFRSF10B (TRAIL receptor DR4 and DR5, respectively) are of particular interest due to their up regulation upon PRKCB inhibition. Previous report on Jurkat or HL-60 human leukemia cell demonstrated that inhibition of PRKCB sensitized tumor cells to TNF-alpha related apoptosis via ligand-induced death receptor (33). Similar mechanisms may occur in Ewing sarcoma and further experiments by both impairing PRKCB and targeting TNF-alpha or NFKB pathways may be required to get deeper insights of PRKCB involvement in these processes.

PRKCB, as a kinase, possesses an enzymatic activity that can be directly targeted and we show here that blocking PRKCB in Ewing sarcoma is a new promising therapeutic approach.

Acknowledgments

We thank Hans Clevers for the generous gift of the pTER and the Tet repressor expression plasmid (pTet-R), Carlo Lucchessi, Karine Laud and David Gentien for their help.

References

1. Aurias A, Rimbaut C, Buffe D, Zucker JM, Mazabraud A. Translocation involving chromosome 22 in Ewing's sarcoma. A cytogenetic study of four fresh tumors. Cancer genetics and cytogenetics. 1984;12(1):21-5.

2. Delattre O, Zucman J, Plougastel B, et al. Gene fusion with an ETS DNA-binding domain caused by chromosome translocation in human tumours. Nature. 1992;359(6391):162-5.

3. Scotlandi K, Benini S, Sarti M, et al. Insulin-like growth factor I receptor-mediated circuit in Ewing's sarcoma/peripheral neuroectodermal tumor: a possible therapeutic target. Cancer Res. 1996;56(20):4570-4.

4. Hancock JD, Lessnick SL. A transcriptional profiling meta-analysis reveals a core EWS-FLI gene expression signature. Cell Cycle. 2008;7(2):250-6.

5. Prieur A, Tirode F, Cohen P, Delattre O. EWS/FLI-1 silencing and gene profiling of Ewing cells reveal downstream oncogenic pathways and a crucial role for repression of insulin-like growth factor binding protein 3. Mol Cell Biol. 2004;24(16):7275-83.

6. Wai DH, Schaefer KL, Schramm A, et al. Expression analysis of pediatric solid tumor cell lines using oligonucleotide microarrays. International journal of oncology. 2002;20(3):441-51.

7. Siligan C, Ban J, Bachmaier R, et al. EWS-FLI1 target genes recovered from Ewing's sarcoma chromatin. Oncogene. 2005;24(15):2512-24.

8. Kinsey M, Smith R, Lessnick SL. NR0B1 is required for the oncogenic phenotype mediated by EWS/FLI in Ewing's sarcoma. Mol Cancer Res. 2006;4(11):851-9.

9. Mendiola M, Carrillo J, Garcia E, et al. The orphan nuclear receptor DAX1 is up-regulated by the EWS/FLI1 oncoprotein and is highly expressed in Ewing tumors. International journal of cancer. 2006;118(6):1381-9.

10. Smith R, Owen LA, Trem DJ, et al. Expression profiling of EWS/FLI identifies NKX2.2 as a critical target gene in Ewing's sarcoma. Cancer cell. 2006;9(5):405-16.

11. Luo W, Gangwal K, Sankar S, Boucher KM, Thomas D, Lessnick SL. GSTM4 is a microsatellite-containing EWS/FLI target involved in Ewing's sarcoma oncogenesis and therapeutic resistance. Oncogene. 2009;28(46):4126-32.

12. Riggi N, Suva ML, De Vito C, et al. EWS-FLI-1 modulates miRNA145 and SOX2 expression to initiate mesenchymal stem cell reprogramming toward Ewing sarcoma cancer stem cells. Genes Dev. 2010;24(9):916-32.

13. Olmos D, Martins AS, Jones RL, Alam S, Scurr M, Judson IR. Targeting the Insulin-Like Growth Factor 1 Receptor in Ewing's Sarcoma: Reality and Expectations. Sarcoma. 2011;2011402508.

14. Baird K, Davis S, Antonescu CR, et al. Gene expression profiling of human sarcomas: insights into sarcoma biology. Cancer research. 2005;65(20):9226-35.

15. Kauer M, Ban J, Kofler R, et al. A molecular function map of Ewing's sarcoma. PLoS ONE. 2009;4(4):e5415.

16. Welford SM, Gregg J, Chen E, et al. Detection of differentially expressed genes in primary tumor tissues using representational differences analysis coupled to microarray hybridization. Nucleic acids research. 1998;26(12):3059-65.

17. Culhane AC, Perriere G, Considine EC, Cotter TG, Higgins DG. Between-group analysis of microarray data. Bioinformatics (Oxford, England). 2002;18(12):1600-8.

18. Fattet S, Haberler C, Legoix P, et al. Beta-catenin status in paediatric medulloblastomas: correlation of immunohistochemical expression with mutational status, genetic profiles, and clinical characteristics. The Journal of pathology. 2009;218(1):86-94.

19. Janoueix-Lerosey I, Lequin D, Brugieres L, et al. Somatic and germline activating mutations of the ALK kinase receptor in neuroblastoma. Nature. 2008;455(7215):967-70.

20. Williamson D, Missiaglia E, de Reynies A, et al. Fusion gene-negative alveolar rhabdomyosarcoma is clinically and molecularly indistinguishable from embryonal rhabdomyosarcoma. J Clin Oncol. 2010;28(13):2151-8.

21. Foell JL, Hesse M, Volkmer I, Schmiedel BJ, Neumann I, Staege MS. Membrane-associated phospholipase A1 beta (LIPI) Is an Ewing tumour-associated cancer/testis antigen. Pediatric blood & cancer. 2008;51(2):228-34.

22. Miyagawa Y, Okita H, Itagaki M, et al. EWS/ETS regulates the expression of the Dickkopf family in Ewing family tumor cells. PloS one. 2009;4(2):e4634.

23. Meynet O, Scotlandi K, Pradelli E, et al. Xg expression in Ewing's sarcoma is of prognostic value and contributes to tumor invasiveness. Cancer research. 2010;70(9):3730-8.

24. Tirode F, Laud-Duval K, Prieur A, Delorme B, Charbord P, Delattre O. Mesenchymal stem cell features of ewing tumors. Cancer cell. 2007;11(5):421-9.

25. Metzger E, Imhof A, Patel D, et al. Phosphorylation of histone H3T6 by PKCbeta(I) controls demethylation at histone H3K4. Nature. 2010;464(7289):792-6.

26. Birney E, Stamatoyannopoulos JA, Dutta A, et al. Identification and analysis of functional elements in 1% of the human genome by the ENCODE pilot project. Nature. 2007;447(7146):799-816.

27. Graff JR, McNulty AM, Hanna KR, et al. The protein kinase Cbeta-selective inhibitor, Enzastaurin (LY317615.HCl), suppresses signaling through the AKT pathway, induces apoptosis, and suppresses growth of human colon cancer and glioblastoma xenografts. Cancer research. 2005;65(16):7462-9.

28. Tirado OM, MacCarthy CM, Fatima N, Villar J, Mateo-Lozano S, Notario V. Caveolin-1 promotes resistance to chemotherapy-induced apoptosis in Ewing's sarcoma cells by modulating PKCalpha phosphorylation. International journal of cancer. 2010;126(2):426-36.

29. Ikner A, Ashkenazi A. TWEAK induces apoptosis through a death-signaling complex comprising receptor-interacting protein 1 (RIP1), Fas-associated death domain (FADD), and caspase-8. J. Biol. Chem. 2011;286(24):21546-21554.[cité2011déc13]

30. Abrams ST, Brown BR, Zuzel M, Slupsky JR. Vascular endothelial growth factor stimulates protein kinase CbetaII expression in chronic lymphocytic leukemia cells. Blood. 2010;115(22):4447-54.

31. Holzer G, Obermair A, Koschat M, Preyer O, Kotz R, Trieb K. Concentration of vascular endothelial growth factor (VEGF) in the serum of patients with malignant bone tumors. Medical and pediatric oncology. 2001;36(6):601-4.

32. Hu-Lieskovan S, Heidel JD, Bartlett DW, Davis ME, Triche TJ. Sequence-specific knockdown of EWS-FLI1 by targeted, nonviral delivery of small interfering RNA inhibits tumor growth in a murine model of metastatic Ewing's sarcoma. Cancer Res. 2005;65(19):8984-92.

33. Meng XW, Heldebrant MP, Flatten KS, et al. Protein kinase Cbeta modulates ligand-induced cell surface death receptor accumulation: a mechanistic basis for enzastaurin-death ligand synergy. The Journal of biological chemistry. 2010;285(2):888-902.

34. R Development Core Team. R: A language and environment for statistical computing.[Internet]. Vienna, Austria.: R Foundation for Statistical Computing; 2006.Available from: http://www.R-project.org.

35. Culhane AC, Thioulouse J, Perriere G, Higgins DG. MADE4: an R package for multivariate analysis of gene expression data. Bioinformatics (Oxford, England). 2005;21(11):2789-90.

36. Dai M, Wang P, Boyd AD, et al. Evolving gene/transcript definitions significantly alter the interpretation of GeneChip data. Nucleic Acids Res. 2005;33(20):e175.[cité2011déc6]

37. Huang DW, Sherman BT, Lempicki RA. Bioinformatics enrichment tools: paths toward the comprehensive functional analysis of large gene lists. Nucleic Acids Res. 2009;37(1):1-13.[cité2011oct3]

38. Subramanian A, Tamayo P, Mootha VK, et al. Gene set enrichment analysis: a knowledge-based approach for interpreting genome-wide expression profiles. Proceedings of the National Academy of Sciences of the United States of America. 2005;102(43):15545-50.

39. Guillon N, Tirode F, Boeva V, Zynovyev A, Barillot E, Delattre O. The oncogenic EWS-FLI1 protein binds in vivo GGAA microsatellite sequences with potential transcriptional activation function. PLoS ONE. 2009;4(3):e4932.

Figure legends

Figure 1. Protein kinase C Beta expression in Ewing tumors

A. Between Group Analysis of expression profiles from five pediatric tumor types. Samples (colored circles) are separated along axes together with probesets (light gray dots) responsible for their separation. Position of probesets corresponding to *NR0B1*, *NKX2-2* and *PRKCB* are emphasized (colored stars).

B. Boxplot of *PRKCB* expression (log2 intensity of affymetrix hgu133plus2 probeset 227817_at) among several pediatric or bone tumors. ET: Ewing tumors; MB: Medullobalstomas; NB: Neuroblastomas; DSRCT: Desmoplastic small round cell tumors; OS: Osteosarcomas; RMS: Rhabdomyosarcomas; SV: Synovial sarcomas

C. Expression of *PRKCB1* and *PRKCB2* in three Ewing cell lines (A673, EW24 and SK-N-MC) as compared to non-Ewing cell lines (HeLa, Jurkat and SJNB1). Beta-actin was used as loading control.

Figure 2. Direct EWSR1FLI1 dependency of *PRKCB* expression

A. Expression of *PRKCB* (isoform 1 and 2) assessed by quantitative RT-PCR on three Ewing cell lines treated with EWSR1FLI1 (siEF1) or control (siCT) siRNA. Means and standard deviation are shown for duplicate experiments.

B. Expression PRKCB2 assessed by Western Blot in different Ewing cell lines inhibited or not for EWSR1FLI1 by siRNA. Beta-actin was used as loading control.

C. EWSR1FLI1 stimulation of *PRKCB* promoter-driven (pREP4-PRKCBprom) luciferase activity in HeLa cells transfected with increasing amount of EWSR1FLI1 (pCDH_EF1) as compared to HeLa cells transfected with empty vectors (pCDH and pREP4). Luciferase activity was normalized by Renilla luciferase activity. Mean and standard deviation of duplicate experiments are shown.

D. EWSR1FLI1 stimulation of *PRKCB* promoter-driven luciferase activity demonstrated in shA673-1C cells treated (+Dox) or not (-Dox) with doxycycline. Luciferase activity was normalized by Renilla luciferase activity. Mean and standard deviation of duplicate experiments are shown.

E. Presence of EWSR1FLI1 on *PRKCB* promoter *in vivo* assessed by chromatin immunoprecipitation using FLI1 antibodies (7.3 or C19) or without antibody as control (-). IP: immunoprecipitated fraction, SN: supernatant.

Figure 3. Synergistic effect of PRKCA and PRKCB for the prevention of histone demethylation in Ewing sarcomas assessed by chromatin immunoprecipitation. Quantitative PCR targeting trimethylated promoter/enhancer regions of known EWSR1FLI1 modulated genes (7 induced and 6 repressed) as well as 6 EWSR1FLI1 unmodulated genes are shown. QPCR values for each gene/CHIP conditions were normalized to their respective input. Means and standard deviations of 2 replicates are shown.

A, C and E: ChIP with an antibody against histone H3T6 phosphorylation (H3T6ph).

B, D and F: ChIP with an antibody against histone H3K4 tri-methylation (H3K4me3).

A and B. A673 cells treated for 72 hours with 6μM of Enzastaurin or with equivalent amount of DMSO.

C and D. A673 cell transfected with siRNA targeting *PRKCB* (siPRKCB) or with non-targeting negative siRNA control (siCT).

E and F. A673 cell transfected with both siRNA targeting *PRKCB* and *PRKCA* (siPRKCA+siPRKCB) or with non-targeting negative siRNA control (siCT).

Figure 4. Crucial importance of PRKCB for *in vitro* Ewing cell survival

A. Cell growth was assessed by MTS assay upon *PRKCB* inhibition by sh463 and sh847 as compared to shCT in three different Ewing cell lines. Means and standard deviations of three independent replicates are shown.

B. Rescue of *PRKCB*-inhibition induced phenotype by expression of mutated PRKCB1 or PRKCB2 ($PRKCB^{463m}$ or $PRKCB^{847m}$) in A673, SK-N-MC and TC71. Means and standard deviations of cell counts over the three cell lines are shown. (-): empty expression vector.

C. Cell death mediated by *PRKCB* inhibition (sh463, light gray) as compared to control cells (shCT, dark gray) assessed by SubG1 population (left panel), cleaved caspase 3 (center panel) and Annexin V presentation (right panel) in three different Ewing cell lines. Welch t-test p-value<0.05 (*) or <0.01 (**). D. Enzastaurin IC50 in three ES cell lines. Growth of A673, SK-N-MC and TC71 Ewing sarcoma cell was determined by cell counting. Cells were treated with increasing concentrations of Enzastaurin (A673: 0, 2.5, 5, 10, 20 and 40 μM; SK-N-MC and TC71: 0, 1, 2, 4, 8, 16 μM) for 72h (plain lines, closed symbols). Control experiments were performed by adding equivalent amount of DMSO to the cells (dashed lines, open symbols). Triangles: A673; circles: SK-N-MC; diamonds: TC71. Means and standard deviations of two experiments are shown.

Figure 5. Crucial importance of PRKCB for *in vivo* Ewing cell survival

A. shA673-B5M3 cells were injected subcutaneously in SCID mice (n=5 mice per group) and doxycycline treatment (plain curve) or sucrose treatment (dashed curve) was started four days after injection.

B. shA673-B5M3 (open circle) or control shA673-pTER (black diamonds) cells were injected subcutaneously in SCID mice (n=5 mice per group) and doxycycline treatment (plain curve) or sucrose treatment (dashed curve) when the mean tumor volume of the group reached $250mm^3$. * Welch t-test p-value < 0.05 between shA673-B5M3 treated with or without Dox at twelve days.

C. A673 cells were injected into tibial muscle of athymic nude mice. Once tumors were measurable, mice were randomly assigned into treatment groups receiving either oral gavage with enzastaurin suspended in olive oil (100mg/kg, twice daily; n = 6) or vehicle alone (n = 7). Welch t-test p-value: * < 0.05, **<0.01

For each panel, average tumor volume and standard deviation are shown

Figure 6. Overlap between EWSR1FLI1, PRKCB and PRKCA modulated genes.

A. Venn diagram showing the overlap between lists of genes modulated by EWSR1FLI1 (EF1vsCT) and PRKCB (PKCBvsCT) siRNAs as compared to a control siRNA experiments, in A673 Ewing cell line. Tables show the modulation direction (up or down regulation) in the overlap.

B. GSEA on genes ranked differentially between siPRKCB and siControl identified signature of TNF, NF-kB and death pathways in PRKCB inhibited samples.

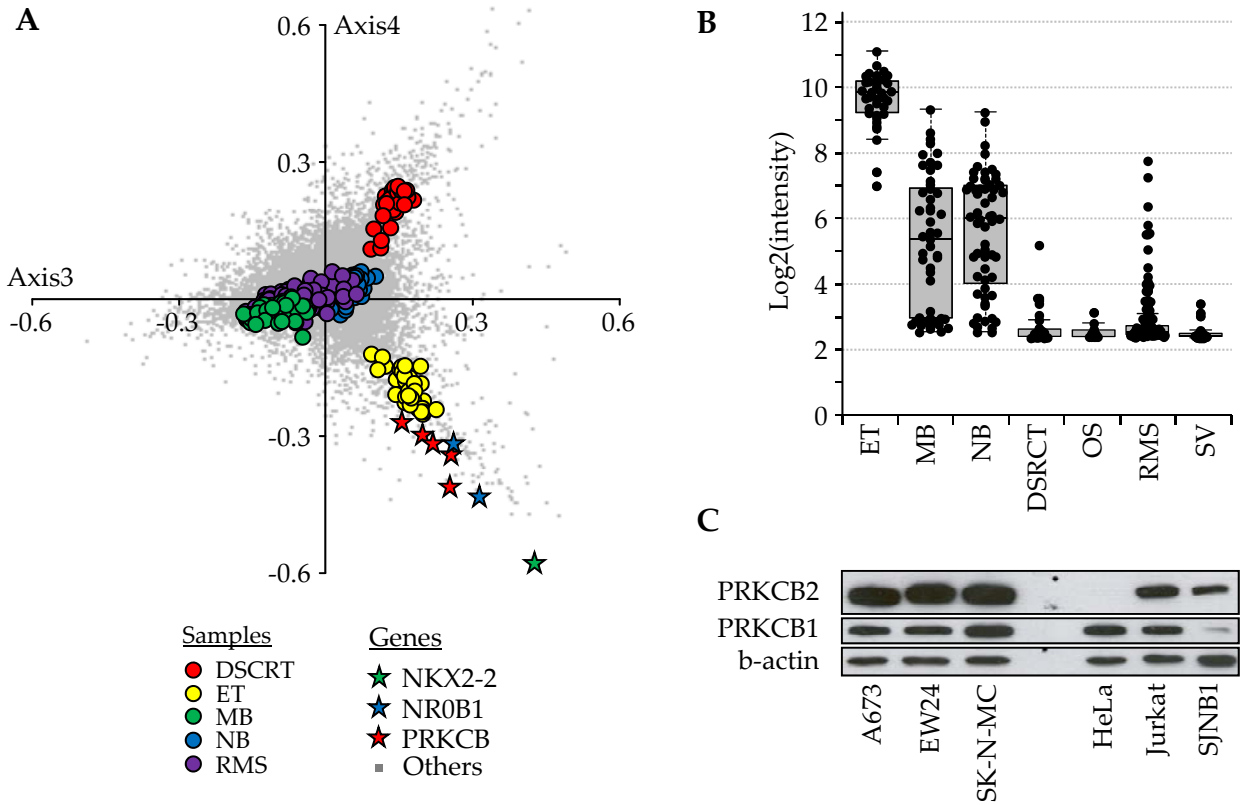

Surdez et al. Figure 1

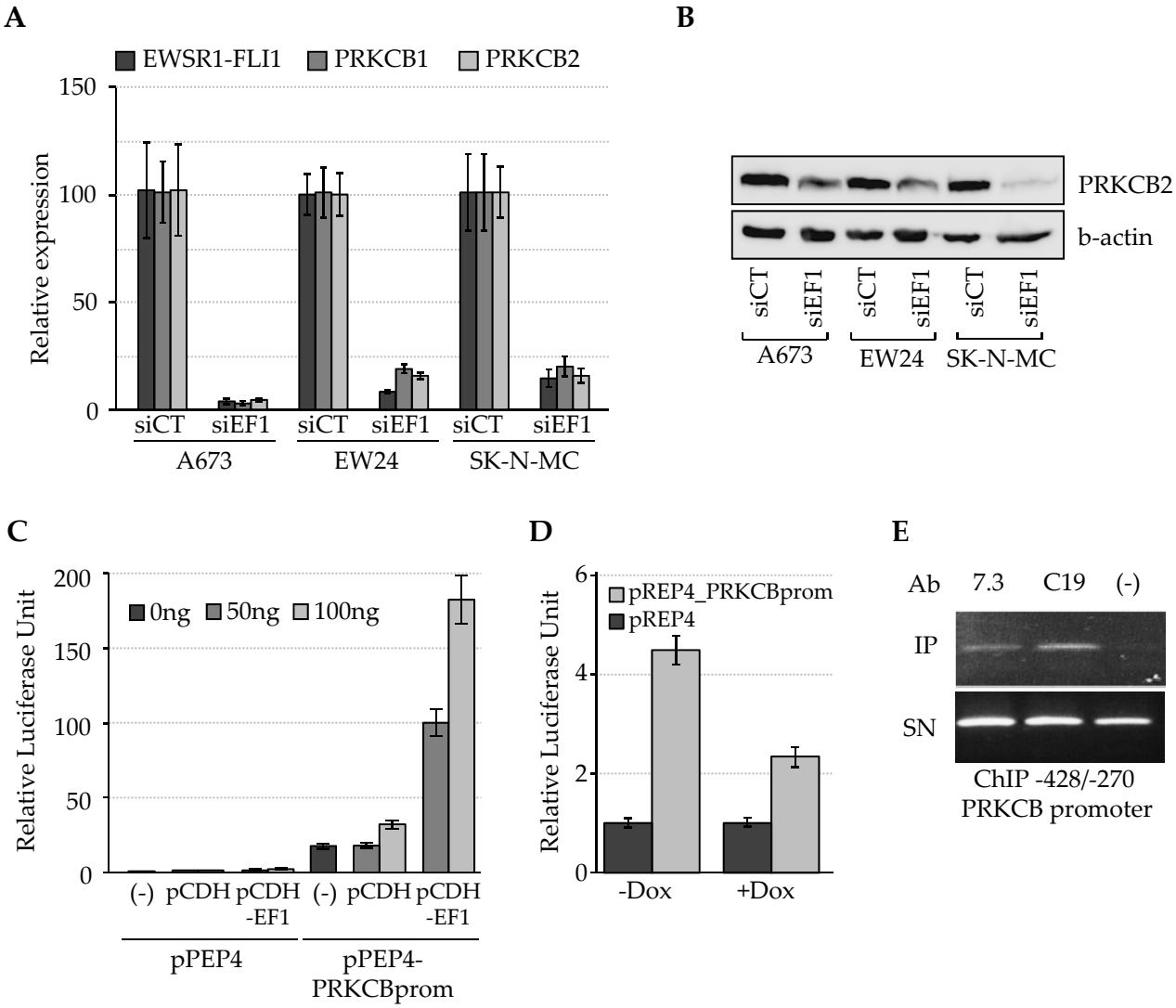

Surdez et al. Figure 2

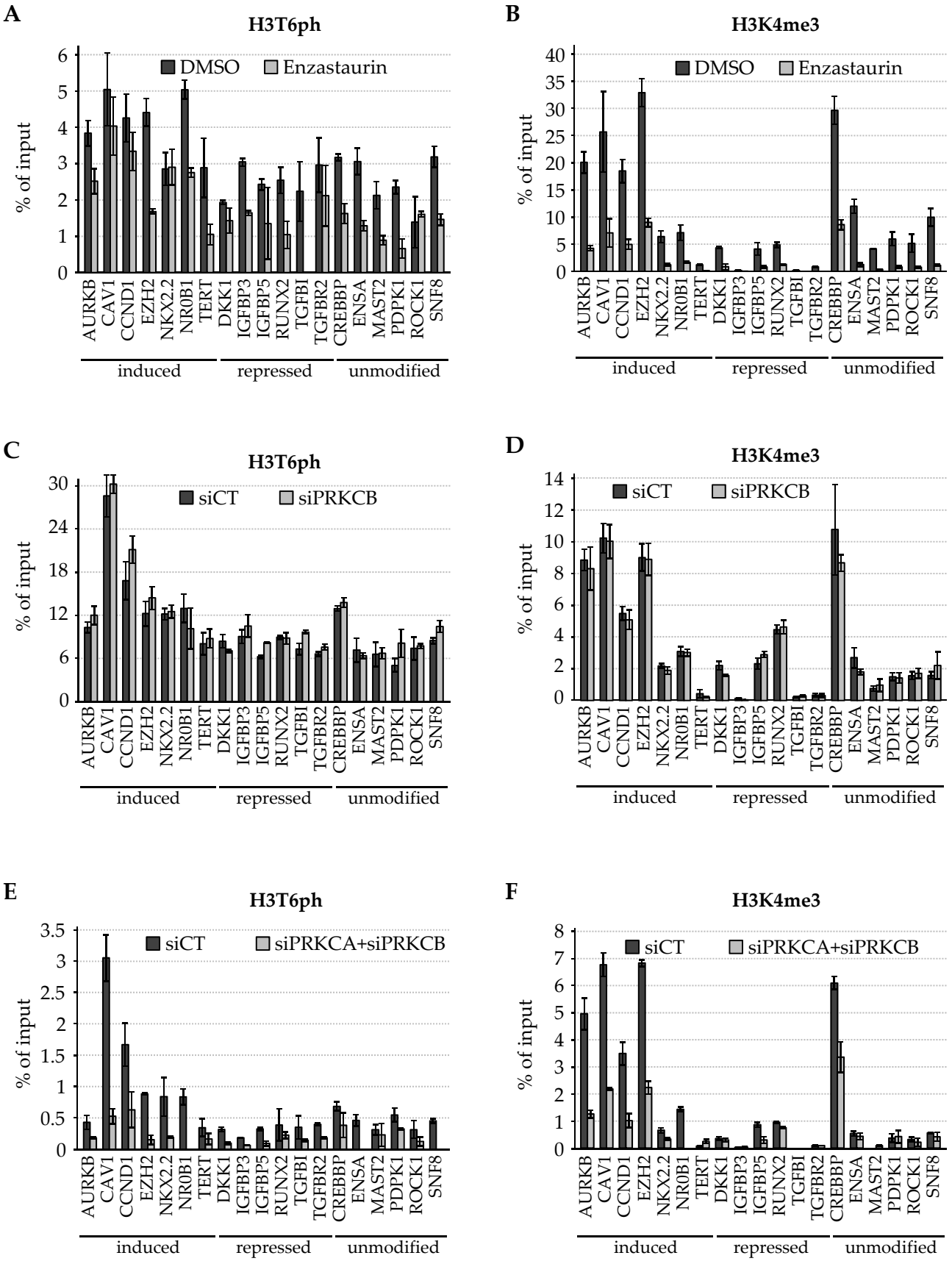

Surdez et al. Figure 3

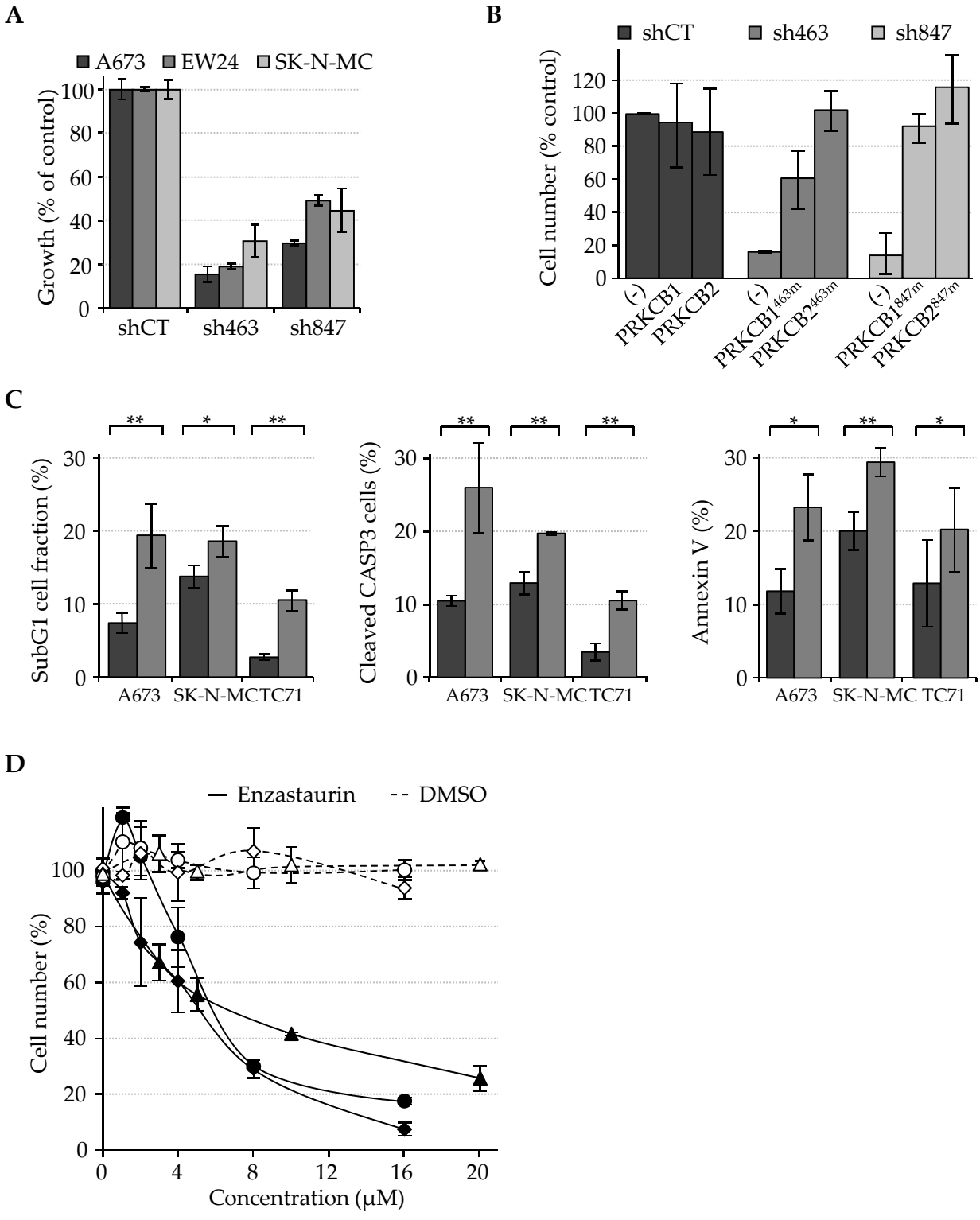

Surdez et al. Figure 4

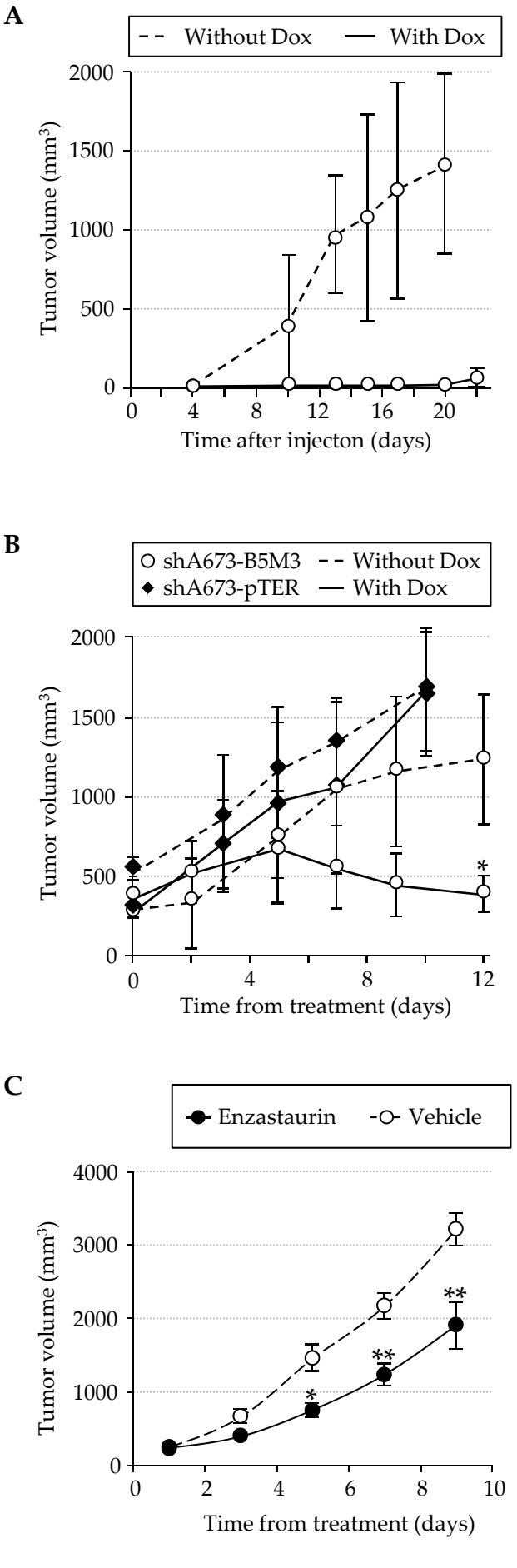

Surdez et al. Figure 5

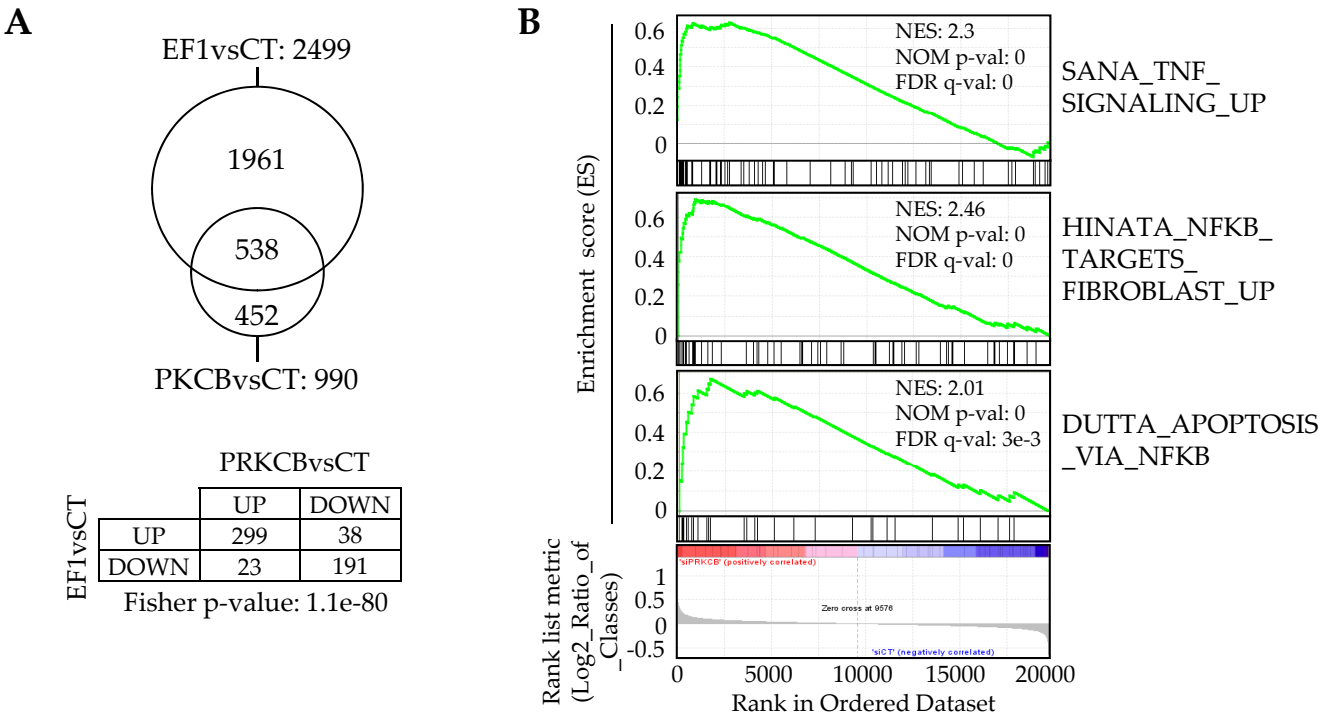

Surdez et al. Figure 6

Supplementary Online Material

Targeting EWSR1-FLI1 oncogene induced protein kinase C beta abolishes Ewing sarcoma growth in vivo

Didier Surdez[1,2], Magdalena Benetkiewicz[1,2], Virginie Perrin[1,2], Zhi-Yan Han[1,2], Gaëlle Pierron[1,3], Stelly Ballet[1,3], François Lamoureux[4,5], Françoise Rédini[4,5], Estelle Daudigeos-Dubus[6,7], Birgit Geoerger[6,7], Olivier Delattre[1,2,3] and Franck Tirode[1,2,*]

[1] Institut Curie, 26 rue d'Ulm, 75248 Paris cedex 05, France

[2] INSERM U830, Unité de Génétique et Biologie des Cancers, Paris, France

[3] Institut Curie, Unité de génétique somatique, Paris, France

[4] LUNAM Universités, Université de Nantes, EA3822 : Laboratoire de Physiopathologie de la Résorption Osseuse et Thérapie des Tumeurs Osseuses Primitives, Nantes, France

[5] INSERM, UMR 957, Nantes, France

[6] Institut Gustave Roussy, Université Paris-Sud XI, 114 rue Edouard Vaillant, 94805 Villejuif, France

[7] Centre National de Recherche Scientifique (CNRS), Laboratoire de Vectorologie et Thérapeutiques Anticancéreuses, UMR 8203, 91405 Orsay, France

* Corresponding author :

Franck Tirode

Unité de Génétique et Biologie des Cancers, INSERM U830, Section de Recherche, Institut Curie, 26 rue d'Ulm, 75248 Paris Cedex 05

Tel: 33 1 56 24 66 83

Fax: 33 1 56 24 66 30

Email : franck.tirode@curie.fr

Materials and Methods

Antibodies. FLI1 (C-19), PKCb1 (C-16) and PKCb2 (C-18) antibodies were purchased from Santa Cruz Biotechnology (Santa Cruz, CA, USA). Histone H3 (Ab1791), Histone H3 tri-methyl K4 (ab1012) and Histone H3 phospho T6 (ab14102) antibodies were purchased from abcam (Cambridge, UK) and b-actin antibody (A-5316) from Sigma-Aldrich (Saint-Quentin Fallavier, France). Anti-FLI-1 antibody (7.3) was described previously (1).

Quantitative RT-PCR. cDNAs were synthesized from 1µg of RNA using the GeneAmp RNA PCR core Kit (Applied Biosystem, Courtaboeuf, France). Quantitative PCR analyses were performed using TaqMan Assays-on-demand Gene expression reagents (Applied Biosystem) with qPCR Mastermix Plus without UNG (Eurogentec, Belgium) or performed using SYBR green (Applied Biosystem). For TaqMan® quantitative RT-PCR, Gene Expression Assays Hs00176998_m1 for *PRKCB* and Hs9999902_m1 for RPLP0 as control were purchased from Applied Biosystem (Courtaboeuf, France). For SYBR green quantitative PCR used primers are listed in supplemental Table S4. Reactions were run on an ABI/PRISM 7500 (Applied Biosystem) and analyzed using the 7500 system SDS software.

Luciferase assay. The -1147/+22 region (corresponding to chr16:23,846,175-23,847,343 of human genome version GRCh37/hg19) around *PRKCB* transcription start site was amplified by PCR from A673 genomic DNA. This fragment was cloned into the XhoI site of the pREP4-luc vector (kindly provided by Keji Zhao). HeLa cells, untreated or doxycycline treated shA673-1C cells for 10 days (2) were plated into twenty-four well plates and grown in DMEM (Invitrogen, Cergy Pontoise, France) supplemented with 10% fetal calf serum. Cells were transfected 24 hours later using lipofectamine and Reagent plus (Invitrogen) with 400 ng of either pREP4-luc or pREP4-(-1147/+22)pPRKCB-luc and 10 ng of pREP7-Rluc, (kindly provided by Keji Zhao) and respectively 0, 50, 100 ng of either pCDH1-MCS1-puro (System

Biosciences, CA) or pCDH1-EWS-FLI1 plasmids (3). Twenty four hours post-transfection, cells were lysed and assayed for luciferase activity using the dual luciferase reporter assay system (Promega, Charbonnieres-les-bain, France) according to the manufacturer's instructions. Firefly activity was normalized to Renilla luciferase activity to adjust differences in transfection efficiency.

Plasmids and cloning. All primers used in this paper are listed in supplemental Table S4. Lentiviral vectors containing shRNA directed against *PRKCB1* (SHGLY-NM_002738) were purchased from Sigma-Aldrich (Saint-Quentin Fallavier, France). *PRKCB2* fragment from PRKCB2 ORFEXPRESS™ Gateway® Shuttle Clone (#GC-T0190, GeneCopoeia, Rockville, MD, USA) was PCR-cloned into pCDH1-MCS1-EF1-Puro lentiviral plasmid (System Bioscience, Montain View, CA, USA). pCDH1_PRKCB1 was constructed from pCDH1_PRKCB2 construct by replacing EcoRV-BamHI fragment with fragment from EcoRV site of *PRKCB1* (1777bp from ATG) to stop codon obtained by RT-PCR using RNA from HeLa cells. For rescue experiments, PRKCB mutants were engineered by introducing two point mutations at shRNA_PRKCB463 ($PRKCB^{463m}$) or shRNA_PRKCB847 ($PRKCB^{847m}$) recognition sites in both pCDH1_PRKCB2 and pCDH1_PRKCB1 using QuikChange II Site-Directed Mutagenesis Kit (Agilent technologies, Germany). For the construction of the inducible clone A673-shPRKCB463_B5M3, primers corresponding to the shRNA_PRKCB463 were annealed and cloned between the *Bgl*II and *Hind*III restriction sites of the pTER vector (4) leading to shPRCKB463_pTER vector.

Rescue of the knockdown phenotype by expression of shRNA-resistant PRKCB. Ewing cells (A673, SK-N-MC and TC71) were first infected with *PRKCB* directed shRNA or control shRNA followed by selection with 1µg/mL puromycin (Invivogen, Toulouse, France) two days after infection. The third day after initial infection, equal numbers of cells from each condition were infected by empty or PRKCB-rescue vector. Cells were counted and proteins extracted three days after second infection. *PRKCB* shRNA rescue experiments were done in duplicates and repeated twice.

Proliferation and apoptosis assays. Cell-cycle analyses were performed by BrdU incorporation as previously described (5). Annexin V/PI staining was performed according to the manufacturer's protocol (Apoptosis detection kit I*;* BD Biosciences, San Diego, USA). Cleaved caspase3 staining (Ab#C8487, Sigma) was performed according to the manufacturer's protocol. Cells were infected either with shCTRL or shPRKCB lentiviruses, selected with puromycin for one week and then subjected to FACS analysis (FACScalibur, BD Biosciences). The data were processed using FlowJo software (Tree Star, Inc.).

Cell culture and shPRKCB inducible cell line. ESFT cell lines A673, EW24, SK-N-MC, and TC71, used in this study were cultured as previously described (2). A673tetR5BIII cells (2), expressing the Tet repressor, were transfected with shPRCKB463_pTER and selected with Zeocin (200 µg/mL) and blasticidine (20 µg/mL). Several clones were isolated and one clone (A673-shPRKCB463_B5M3) exhibiting strong inhibition of *PRKCB* upon induction with 2 µg/mL Doxycycline was selected. As a control, A673tetR5BIII cells were also transfected with empty pTER vector and a population resistant to zeomycin and blasticidin was selected (shA673-pTER cells).

siRNA experiments. The following Stealth siRNA (Invitrogen) were used (sens primers only): siPRKCA: 5'-gccuccauuugauggugaagaugaa-3'; siPRKCB: 5'-aaugcaugcucuuugauaucacguu-3'; Stealth *RNAi* Negative Control Low GC (Invitrogen) was used as a negative control. Cells were transfected for 72h with 50nM of stealth siRNA using Lipofectamine RNAiMAX (Invitrogen) according to manufacturer's recommendations.

Supplemental References

1. Melot T, Gruel N, Doubeikovski A, Sevenet N, Teillaud JL, Delattre O. Production and characterization of mouse monoclonal antibodies to wild-type and oncogenic FLI-1 proteins. Hybridoma. 1997;16(5):457-64.
2. Tirode F, Laud-Duval K, Prieur A, Delorme B, Charbord P, Delattre O. Mesenchymal stem cell features of ewing tumors. Cancer cell. 2007;11(5):421-9.

3. Guillon N, Tirode F, Boeva V, Zynovyev A, Barillot E, Delattre O. The oncogenic EWS-FLI1 protein binds in vivo GGAA microsatellite sequences with potential transcriptional activation function. PLoS ONE. 2009;4(3):e4932.
4. van de Wetering M, Oving I, Muncan V, et al. Specific inhibition of gene expression using a stably integrated, inducible small-interfering-RNA vector. EMBO Rep. 2003;4(6):609-15.
5. Dauphinot L, De Oliveira C, Melot T, et al. Analysis of the expression of cell cycle regulators in Ewing cell lines: EWS-FLI-1 modulates p57KIP2and c-Myc expression. Oncogene. 2001;20(25):3258-65.

Author contributions

FT, DS, MB and OD conceived the study. DS, FT, MB, VP, ZH performed the experiments and analyzed the data. GP and SB were involved in tumors processing and microarrays. EDD, BG, FL and FR performed in vivo drug experiments. DS, FT and OD wrote the paper.

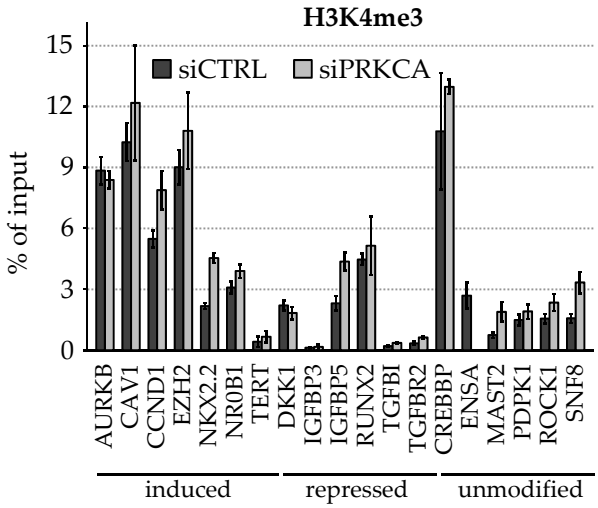

Supplemental Figure S1. Single inhibition of PRKCA does not reduce the global level of histone H3K4 tri-methylation (H3K4me3). A673 Ewing sarcoma cell were transfected with siRNA targeting PRKCA or non-targeting negative siRNA control. 3 days after transfection, cells were fixed and processed for CHIP using antibodies against histone H3K4 tri-methylation (H3K4me3). Quantitative PCR targeting trimethylated promoter/enhencer regions of known EWSR1FLI1 modulated genes (7 induced and 6 repressed) as well as 6 EWSR1FLI1 unmodulated genes. QPCR values for each gene/CHIP conditions were normalized to their respective input.

A

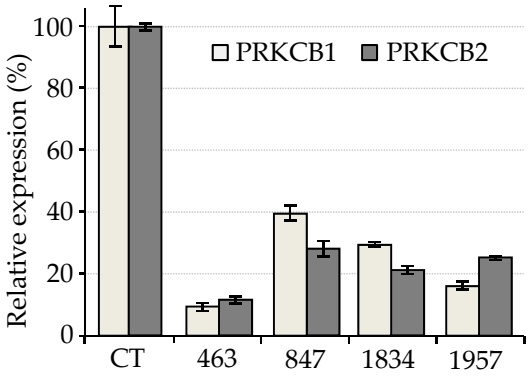

B

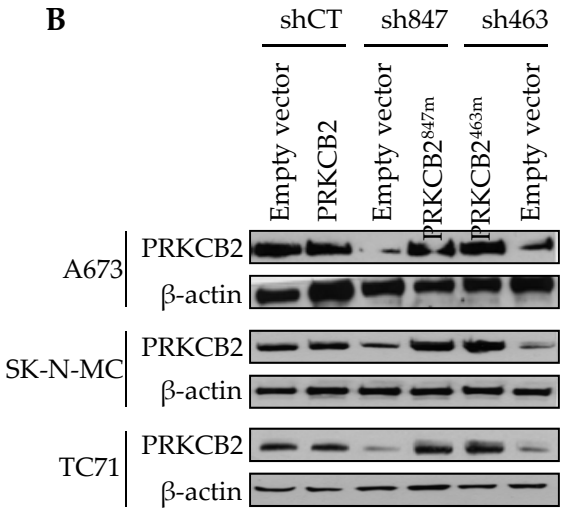

C

```
sh463            ...C AAG TTT AAG ATC CAC ACG TAC...
                   | ||| ||| ||| ||| ||| ||| |||
PRKCB       461 CAC AAG TTT AAG ATC CAC ACG TAC 484
                ||| ||| ||| ||| ||  ||  ||| |||
PRKCB463m   461 CAC AAG TTT AAG Ata Cat ACG TAC 484

Amino Acid      H   K   F   K   I   H   T   Y


sh847            ...G CTG AAA GAA TCG GAC AAA GAC...
                   | ||| ||| ||| ||| ||| ||| |||
PRKCB       845 CAG CTG AAA GAA TCG GAC AAA GAC 868
                ||| ||  ||  ||| ||| ||| ||| |||
PRKCB847m   845 CAG CTt Aag GAA TCG GAC AAA GAC 868

Amino Acid      Q   L   K   E   S   D   K   D
```

Supplemental Figure S2. Inhibition of PRKCB by shRNAs. **A**. A673 cells were treated with lentiviral particles containing either control or 4 different PRKCB specific shRNAs (numbers indicate the first nucleotide position of PRKCB2 mRNA (NM_002738.3) targeted by the different shRNAs). RT-QPCR were then performed on RNA extracted 5 days post-infection. Error bars represent standard deviations over three independent replicates. **B**. Rescue of PRKCB inhibition. Western blot showing levels of PRKCB2 upon inhibition by PRKCB specific shRNAs (sh463 and sh847) and re-expression of PRKCB2 carrying two silent mutations in the shRNA binding region (847m or 463m). **C**. Sequences alignment of shRNAs, wildtype and point mutated PRKCB and resulting amino acid sequence.

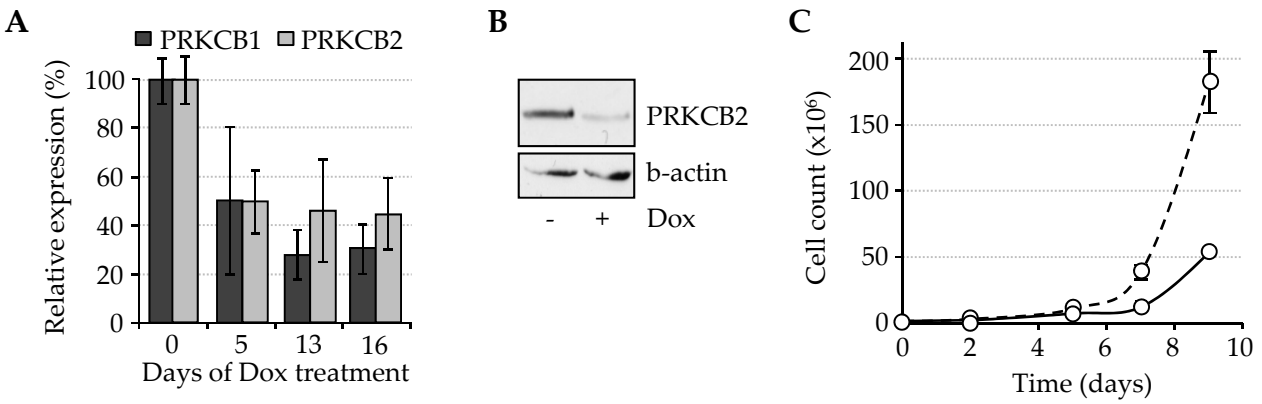

Supplemental Figure S3. Stable A673-shPRKCB463_B5M3 cell line. A. Stable inhibition of *PRKCB1* and *PRKCB2* assessed by RT-QPCR at different time points during doxycycline treatment in A673-shPRKCB463_B5M3 clone (shA673-B5M3). B. Western blot showing PRKCB2 protein level in shA673-B5M3 clone treated with (+) or without (-) doxycycline. Beta-actin is used as loading control. C. *In vitro* cell growth of shA673-B5M3 when treated (plain curve) or not (dashed curve) with doxycycline.